GAMMA TOMOGRAPHIC VISUALIZATION OF THE FLUID DISTRIBUTION IN A HYDRODYNAMIC COUPLING

Dietrich Hoppe, Juergen Fietz, Uwe Hampel, Horst-Michael Prasser, Cornelius Zippe, Karl-Heinz Diele[1], and Reinhard Kernchen[1]

1. Introduction

Gamma tomography is a useful tool for the investigation of single and multiphase flow phenomena. In particular, when phase distributions and flow patterns are to be assessed non-invasively in opaque containments, it is often the only applicable and most reliable method [1], [2]. In the past few years, a gamma tomography apparatus has been developed at the Institute of Safety Research at Research Center Rossendorf which can be used to visualize quasi-stationary fluid distributions in rotating hydromachines, such as axial pumps, mixers, turbines or hydrodynamic couplings [3]. The characteristic principle of the system is the acquisition of tomographic projections in synchronization with the rotation cycle of the investigated object [4]. Furthermore, the approach is based on a difference imaging principle where the distribution of the radiologically less absorptive fluid is reconstructed from a difference measurement of the empty machine and the machine at load. In that way, the absorption contribution of the radiologically dense material of the machine body itself is eliminated before reconstruction resulting in clean slice images of the interesting fluid distribution.

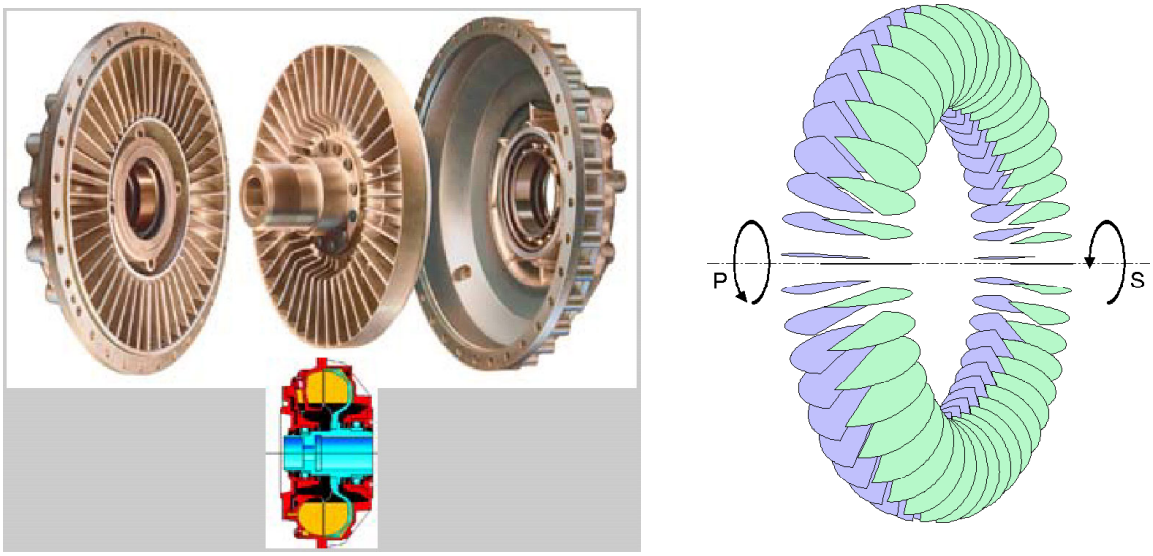

Fig. 1: Assembly and functional principle of a hydrodynamic coupling.

[1] Voith Turbo GmbH Crailsheim

2. Hydrodynamic couplings

Hydrodynamic couplings serve as torque conversion elements in heavy load rotating drive systems and can be found in numerous technical systems such as power plants, naval vessels, railed vehicles, busses and trucks. [5]. They use the principle of torque conversion by means of a fluid – a principle that is superior to other coupling mechanisms in terms of conversion efficiency, smooth transient behavior, low material deterioration and thus long durability.

The functional principle of a hydrodynamic coupling is described in Fig. 1. The coupling comprises a metal housing and two axially supported bladed wheels which oppose each other. In the presence of a coupling fluid, which is oil in most cases but may also be water, a torque is transferred from the rotating primary wheel (P) to the secondary wheel (S). Thereby, the rotational speed n_S is lower than the rotational speed n_P, which is referred to as the slip $S = 1 - n_S / n_P$. The conversion of power in a hydrodynamic coupling depends on the geometry and design of the coupling elements (distance of the bladed wheels, number, shape, and arrangement of the blades) and on the filling level F. The latter may be used to realize the coupling function, i. e., the smooth coupling and decoupling of engine and load by varying F with a filling control system.

An optimization of the static and transient behavior of a hydrodynamic coupling in operation is mainly achieved by thorough design of the coupling elements. However, to assess the interrelation of flow patterns, torque conversion characteristics and coupling design it is required to look inside the coupling during operation. One way to achieve this is to build test couplings with optically clear housing parts for visual inspection. However, optical methods such as stroboscopic video imaging give poor information on the fluid volume distribution due to multiple reflection and refraction of light at the phase boundaries. They also require larger manufacturing effort and provide less flexibility to the experimenter since the design of the test coupling and its surroundings must be accommodated to the needs of visual inspection. One aim of the reported work was thus to initially prove the applicability of gamma tomography to the diagnostics of flow phenomena in hydrodynamic couplings.

3. Tomographic measurement system

The Rossendorf gamma tomograph is shown in Fig. 2 as it was installed at the hydrodynamic coupling test facility at Voith Turbo GmbH in Crailsheim. The system consists of a Cs-137 source with an overall activity of $1{,}85 \cdot 10^{11}$ Bq, a detector arc, a tomograph gantry, a control and data acquisition unit, and a measurement PC. The gamma source is a cylindrically shaped capsule with a diameter of 5,8 mm and a length of 11,9 mm contained in a double-welded stainless steel envelope which in turn resides in a shielded working container. The source can be manually driven to the working position by means of a bowden cable. A collimator that is mounted in front of the source container provides a spatial limitation of the gamma radiation to an angle of 60° within the measurement plane and 10° axial. The detector arc is mounted on the gantry in a distance of 1200 mm away from the source. It consists of 64 consecutively arranged BGO crystals with 1 cm x 1 cm active area and 3 cm depth. The scintillation light is converted to electrical pulses by photomultipliers (one per crystal) which are further processed by proper analog electronics, comprising a pulse forming amplifier and an energy discrimination stage which excludes the scattered events from the data. A subsequent digital electronics counts the valid events of each detector in hardware. Additionally, the measurement PC acquires the signals from two zero-angle transmitters at the primary and the

secondary coupling shaft. The source container and the detector arc are mounted in horizontal position on the tomograph gantry which itself resides on sliding rails such that the whole system can be manually moved to a desired axial scanning plane. The test coupling itself is in the center of this arrangement.

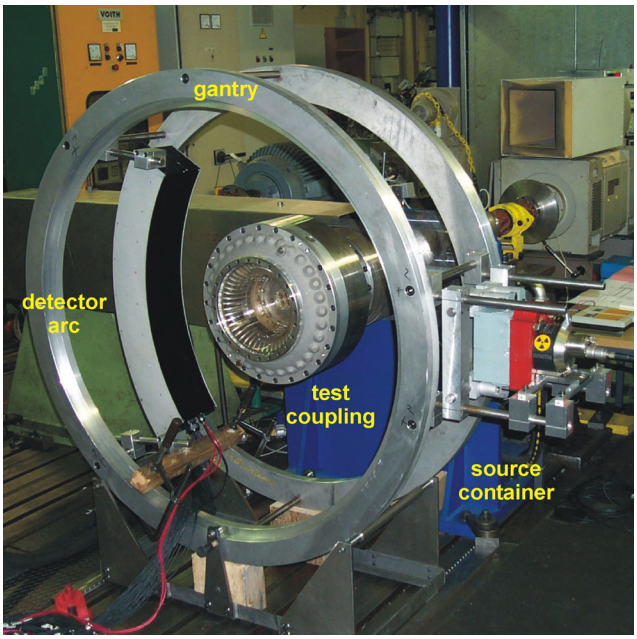

Fig 2: Gamma tomograph at the coupling test facility.

The tomographic reconstruction principle requires the measurement of the integral radiological density for the 64 spatial channels defined by the source and the detector elements and for a number of equally spaced rotation angles. To achieve the angular resolution the counting of valid detector events is limited to intervals of approximately $T = 100$ µs. From the counter values obtained at these intervals a sinogram is built whose number of projection angles is defined by the time per rotation, obtained from the zero-angle transmitter, devided by T. The resulting count number sinogram is further processed to a data set suitable for image reconstruction. From the linear relationship

$$N = N_0 \exp\left(- \int_{source}^{detector} \mu_{Fluid}(s)\, ds \right) \tag{1}$$

with N_0 denoting the count number at a given detector and angular interval for an empty coupling, N the corresponding count number for a coupling partly filled with fluid, and μ_{Fluid} the mass extinction coefficient distribution of the fluid along the ray path parameterized by s it follows, that the integral extinction value E, which is the input data for image reconstruction, is calculated as

$$E = \ln N_0 - \ln N\,. \tag{2}$$

The overall spatial resolution of system is mainly limited by the size of the source and the detector elements. From experiments we have determined the resolution to be about 5 - 6 mm in the vicinity of the object's center.

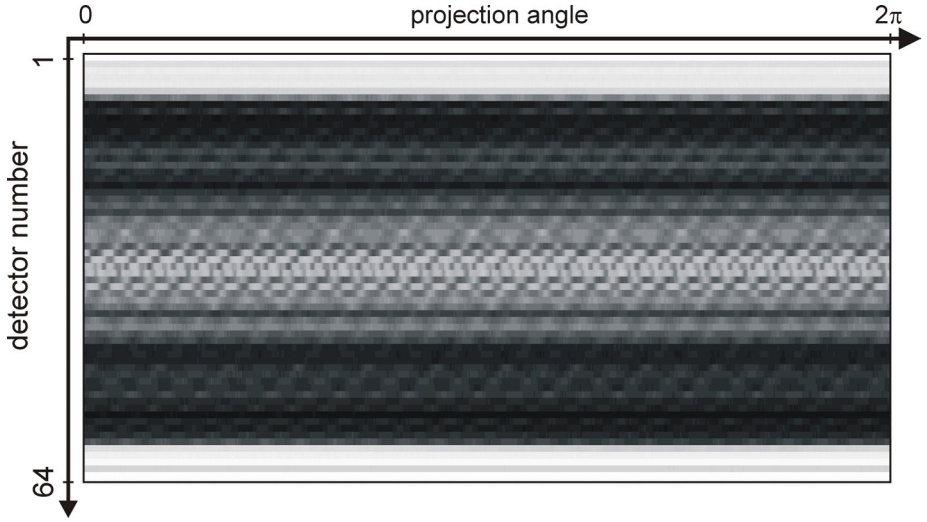

Fig. 3: Normalized gray value represenation of a count number sinogram.

4. Image reconstruction

For image reconstruction, we applied the method of filtered backprojection [6] which we will only briefly sketch in the following. The two-dimensional object space in the tomographic plane has been divided into 491 x 491 square pixels with 1.1 mm edge length. With this discrete representation the image reconstruction process can be formally described as an algebraic operation that reconstructs the fluid mass extinction coefficient μ_{ij} in each pixel *(i,j)*. With the μ_{ij} lumped together in the object vector $\boldsymbol{\mu}$ and the sinogram data in the data vector $\mathbf{m}$ and furthermore introducing the projection matrix $\mathbf{A}$ which contains the geometric area contributions of each pixel to each projection channel, the discrete backprojection is defined by the transformation

$$\mathbf{b} = \mathbf{A}^T \mathbf{m} \tag{3}$$

giving the backprojection image $\mathbf{b}$. This backprojection image is processed to the original object distribution by application of the reconstructing filter matrix $\mathbf{H}$ with

$$\boldsymbol{\mu} = \mathbf{H}\,\mathbf{b} = \mathbf{H}\,\mathbf{A}^T \mathbf{m}\,. \tag{4}$$

The ideal reconstruction operator is given by the discrete Fourier inverse of the two-dimensional ramp filter [6]. However, to avoid image degradation by the present data noise this filter is modified with an apodising cosine window. To increase computational efficiency the deconvolution in equ. 4 is realized by a matrix multiplication in the Fourier domain.

5. Results

A complex experimental program has been carried out to acquire data from different axial planes and operating points of the test coupling. Performing a single scan thereby comprised the following experimental steps:

- selection of the axial plane by manual positioning of the tomograph;
- driving the hydrodynamic test coupling into its operational state (filling level, primary angular speed, secondary angular speed);
- acquisition of projection data over 300 seconds.

This procedure has been repeated for an overall number of 179 tomographic scans. The region of most interest within the hydrodynamic coupling are the chambers formed by the blades of the primary and secondary wheel. Within this region a number of six axial measurement planes has been selected for experimental investigation (Fig. 4). The reconstruction of the cross-sectional image of one such plane (plane no. 3) is illustrated in Fig. 5. The two top images are the reconstruction results for the test coupling with no water (a) and for a water level of F=0.3 (b) at S=0. In both images the material structures of the coupling elements, such as blades and mounting holes, are clearly shown. The water phase is recognized as a dim ring at the outer bladed region. The reconstruction from the difference sinogram is shown in Fig. 5c. Here all invariant image details are cancelled out and the annular water phase is clearly displayed. In Fig. 5d the same reconstruction result is displayed in color for clarity and a scale is provided which indicates the calculated water content of each pixel. Although the fluid distribution is clearly reconstructed, there are also some image distortions to be recognized. Thus, the granularity of actually homogeneous object regions results from statistical noise and background scattering. Partial volume effects combined with the low-pass filtering at the reconstruction stage lead to smooth fluid distribution gradients at the far radius of the fluid annulus where sharp gradients would be expected. Another resolution-related artifact is the appearance of “continuation of the blades and chambers” into the inner section where the test coupling is actually hollow.

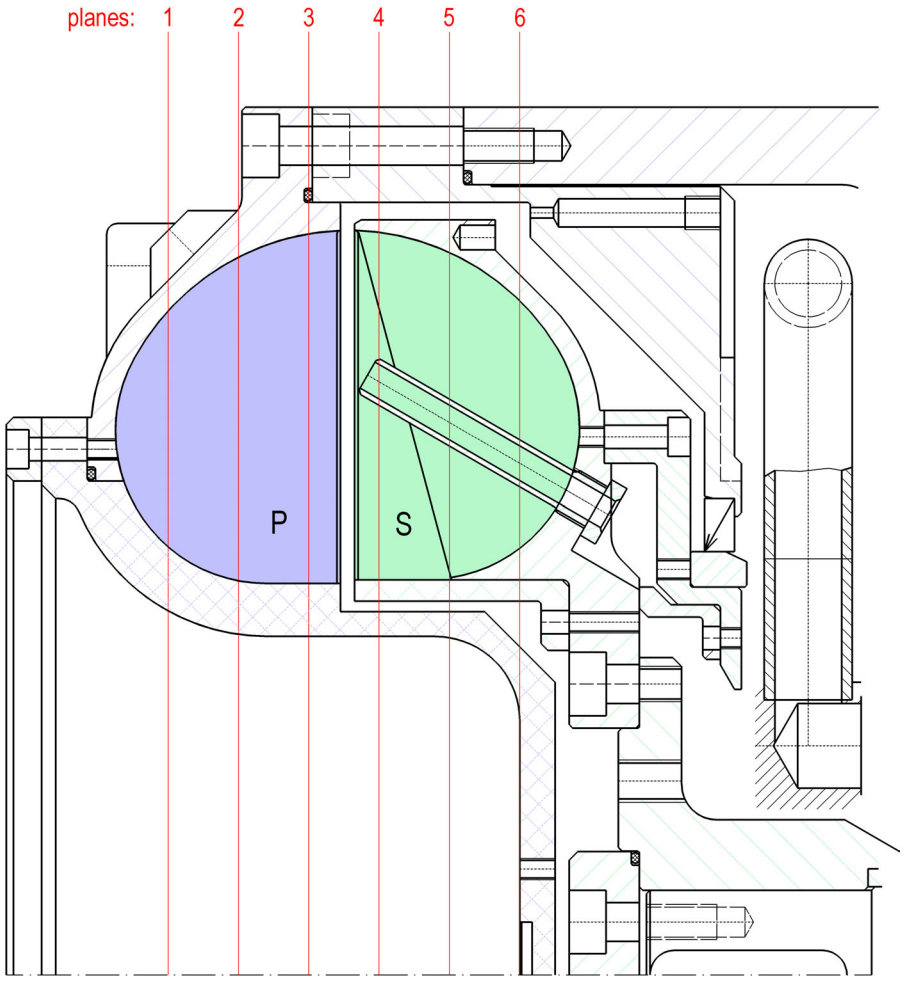

Fig. 4: Axial cross-section of the blades with position of the tomographic planes.

Fig. 6 shows the image stack for all reconstructed slices. From a set of such 2D images taken for the test coupling at F=0.3 and S=0.75 a three-dimensional fluid distribution has been fused, showing the mean volume distribution of the coupling fluid for both primary and secondary side, each reconstructed according to its own angular speed. It should be noted, that only fluid dynamic processes with the angular speed equal to the that of the blades are sharply mapped. Other quasi-stationary components of the flow, which may for example extend from one side into the other are to some degree blurred. Furthermore, it should be mentioned, that the varying mass fraction of the material within the tomographic planes currently limits the absolute accuracy of the fluid mass coefficient reconstructed with the filtered backprojection method which brings about some problems when fusing images of different slices together.

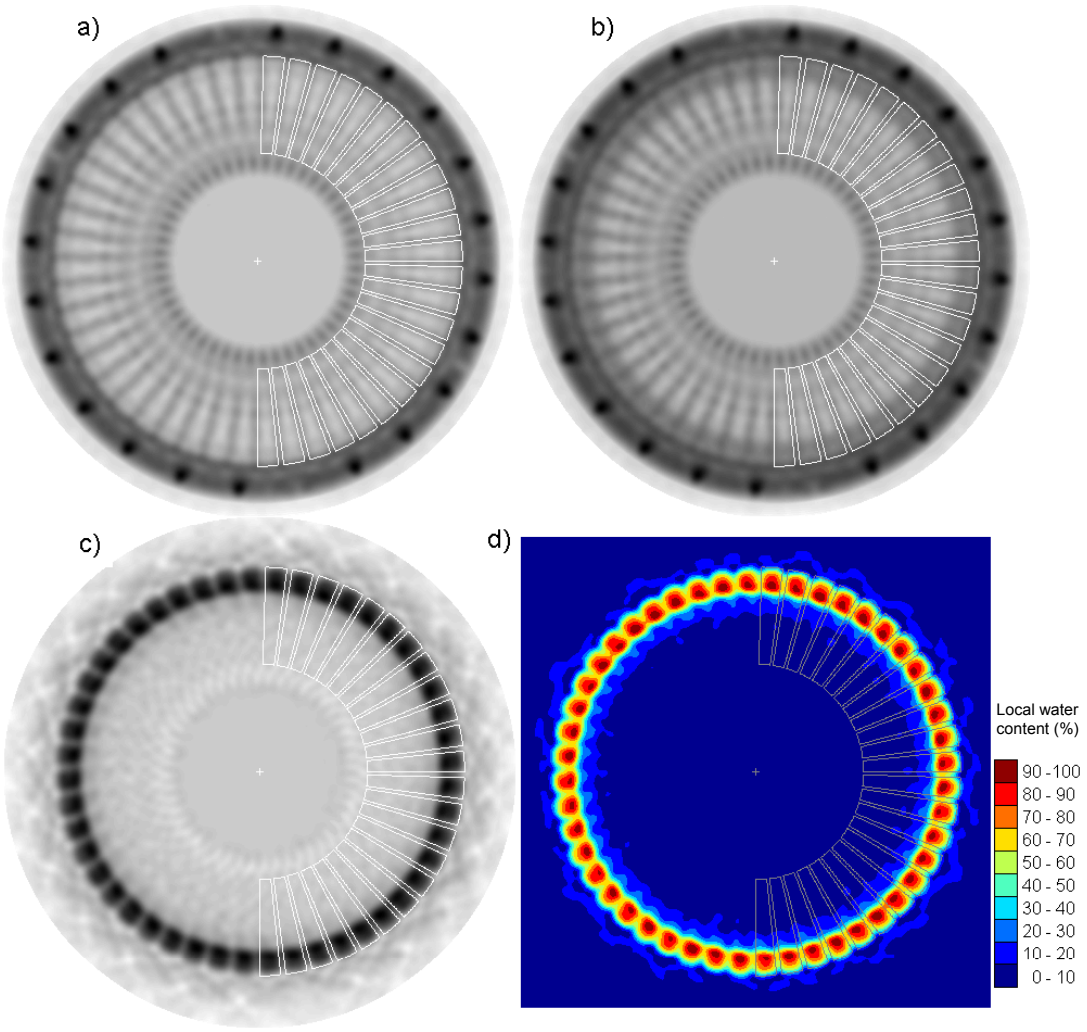

Fig. 5: Reconstructed images of slice no. 3 for the test coupling at S=0. a) Empty coupling (F=0.0), b) filled coupling with F=0.3, c) difference image showing the water distribution, d) color image of c).

6. Discussion

The method of gamma tomography has been used to visualize quasi-stationary fluid distributions in the primary and secondary chamber system of a hydrodynamic coupling in different modes of operation. The reconstructed images give a considerable amount of

information on the interrelation of the coupling design and the local transfer of kinetic energy between the bladed wheels, which may by useful to optimize the design and layout of the coupling elements for specific applications. Though gamma tomography proved to be highly successful for this application remaining problems to be solved in the future are the improvement of spatial resolution and an increase of accuracy in the reconstructed absolute extinction values which may be achieved by iterative image reconstruction algorithms.

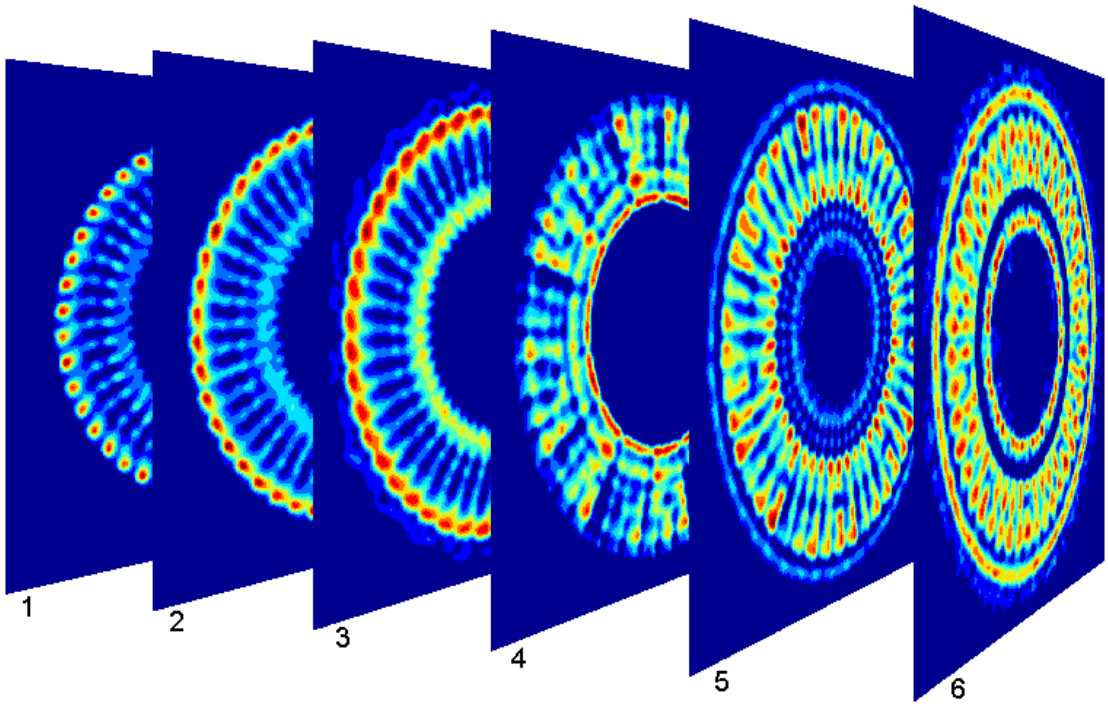

Fig. 6: Series of reconstructed images for the six consecutive axial planes shown in Fig. 4.

References

[1] A. C. Devuono, P. A. Schlosser, F. A. Kulacki, P. Munshi, "Design of an isotopic CT scanner for two-phase flow measurements", IEEE Trans. Nuclear Science, **NS-27,** 1980.

[2] T. Frøystein, "Flow imaging by gamma-ray tomography: data processing and reconstruction techniques, systems", in *Frontiers in Industrial Process Tomography II*, 8–12.4.97, Delft (NL), pp. 185–187, 1997

[3] H.-M. Prasser, D. Baldauf, J. Fietz, U. Hampel, D. Hoppe, C. Zippe, J. Zschau, M. Christen, G. Will, "Time resolving gamma-tomography for periodically changing gas fraction fields and its application to an axial pump", to be published in Flow Meas. and Instrument., 2003.

[4] H.-M. Prasser, J. Zschau, "Anordnung zur messtechnischen Erfassung einer Projektion des Strahlabsorptionsvermögens eines periodisch veränderlichen Messobjektes", Erfindungsanmeldung Az. 101 17 569.8, 1999.

[5] H. Höller, „Hydrodynamische Kupplungen mit konstanter Füllung", Publikation der Voith Turbo GmbH & Co. KG, Crailsheim.

[6] A. C. Kak and M. Slaney. *Principles of Computerized Tomographic Imaging*. IEEE Press, New York, 1987.